Bayesian Study of Nuclear Shapes at the LHC

Govert Nijs

January 13, 2025

Based on:

- GN, van der Schee, 2112.13771, 2206.13522, 2304.06191, 2312.04623
- Giacalone, GN, van der Schee, 2305.00015, xxxx.xxxxx

The status of the field

- The general picture of the stages of a heavy ion collision is known.
- Theoretical modelling follows these stages:
  - T$_R$ENTo or IP-Glasma for the initial state.
  - Free streaming for the pre-hydrodynamic stage.
  - Viscous hydrodynamics with temperature dependent shear and bulk viscosity.
  - SMASH or UrQMD as a hadronic afterburner.
- Recently also: modelling of the projectiles themselves.

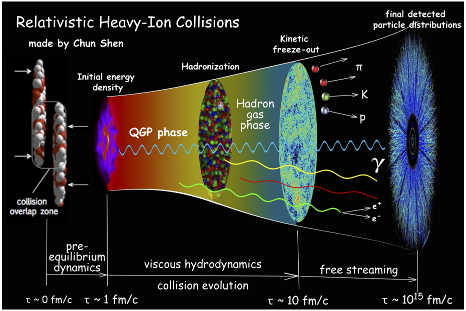

Some basic observables

- Charged particle multiplicity dN/dy. Correlates with how much entropy is produced in the initial state.
  - Centrality is determined by multiplicity percentiles.
- Mean transverse momentum $\langle p_T \rangle$. Sensitive to how much the fluid is being pushed out, i.e. the pressure.
- Anisotropic flow v_n. Defined as azimuthal Fourier coefficients:

$$N(\phi) \propto \sum_n v_n \cos(n(\phi - \Psi_n)).$$

Sensitive to the initial state spatial anisotropy.

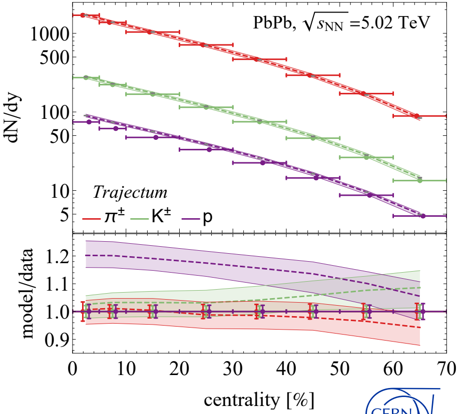

Some basic observables

- Charged particle multiplicity dN/dy. Correlates with how much entropy is produced in the initial state.
  - Centrality is determined by multiplicity percentiles.
- Mean transverse momentum $\langle p_T \rangle$. Sensitive to how much the fluid is being pushed out, i.e. the pressure.
- Anisotropic flow v_n. Defined as azimuthal Fourier coefficients:

$$N(\phi) \propto \sum_n v_n \cos(n(\phi - \Psi_n)).$$

Sensitive to the initial state spatial anisotropy.

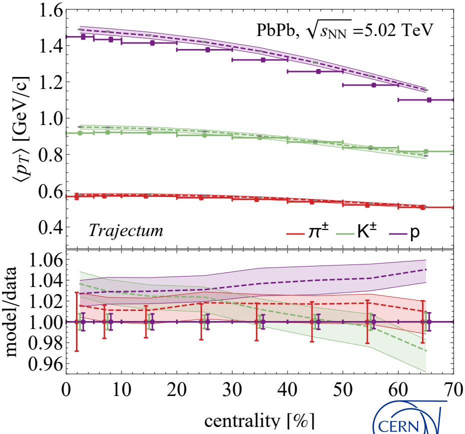

Some basic observables

- Charged particle multiplicity dN/dy. Correlates with how much entropy is produced in the initial state.
  - Centrality is determined by multiplicity percentiles.
- Mean transverse momentum $\langle p_T \rangle$. Sensitive to how much the fluid is being pushed out, i.e. the pressure.
- Anisotropic flow v_n. Defined as azimuthal Fourier coefficients:

$$N(\phi) \propto \sum_n v_n \cos(n(\phi - \Psi_n)).$$

Sensitive to the initial state spatial anisotropy.

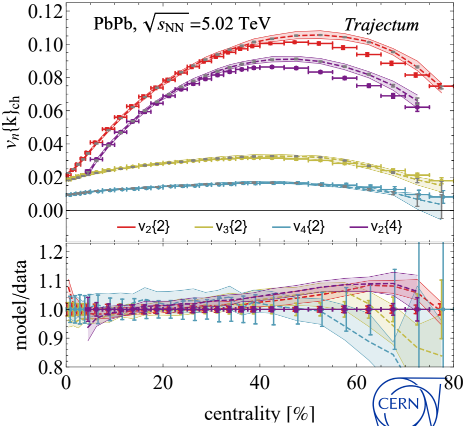

Model used: *Trajectum*

- New heavy ion code developed in Utrecht/MIT/CERN.
  - *Trajectum* is the old Roman name for Utrecht.
- Contains initial stage, hydrodynamics and freeze-out, as well as an analysis suite.
- Easy to use, example parameter files distributed alongside the source code.
- Fast, fully parallelized.
  - Figure (20k oversampled PbPb events at 2.76 TeV) computes on a laptop in 21h.
  - Bayesian analysis requires $\mathcal{O}(1000)$ similar calculations to this one.
- Publicly available at sites.google.com/view/govertnijs/trajectum/.

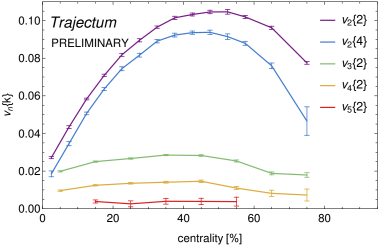

Some simple intuition

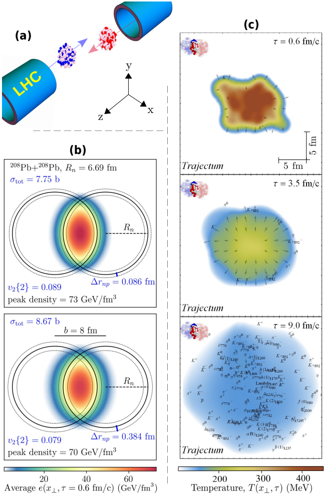

- Model details are not necessary to understand the contents of this talk.
  - We will only discuss small aspects as needed (more details in backup slides).
  - Model parameters will be colored green where they appear.
- Hydrodynamics can be intuitively understood:
  - Pressure gradients drive expansion.
  - Hotter systems expand faster, resulting in more transverse momentum.
  - Spatially anisotropic systems expand preferentially along the short axis, resulting in momentum anisotropy in the final state.

Effects of nuclear structure on soft observables

- The STAR isobar run sparked great interest in nuclear structure in heavy ion collisions.
    - Originally intended to measure the chiral magnetic effect.
- Differences in the shapes of $^{96}_{44}$Ru and $^{96}_{40}$Zr lead to different shape of the initial fireball.
    - We can distinguish several possibilities for the shapes of $^{96}_{44}$Ru and $^{96}_{40}$Zr, with model 5 giving the best agreement.
    - Isobar nature of $^{96}_{44}$Ru and $^{96}_{40}$Zr leads to robust ratios insensitive to details of hydrodynamics.

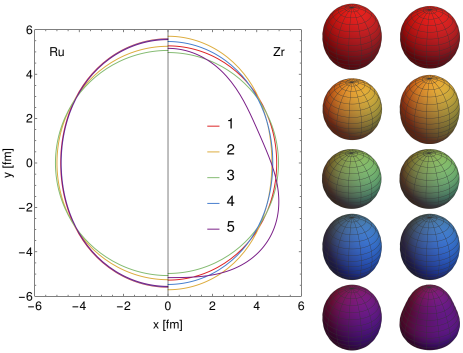

[GN, van der Schee, 2112.13771; STAR, 2109.00131]

Effects of nuclear structure on soft observables

- The STAR isobar run sparked great interest in nuclear structure in heavy ion collisions.
  - Originally intended to measure the chiral magnetic effect.
- Differences in the shapes of $^{96}_{44}$Ru and $^{96}_{40}$Zr lead to different shape of the initial fireball.
  - We can distinguish several possibilities for the shapes of $^{96}_{44}$Ru and $^{96}_{40}$Zr, with model 5 giving the best agreement.
  - Isobar nature of $^{96}_{44}$Ru and $^{96}_{40}$Zr leads to robust ratios insensitive to details of hydrodynamics.

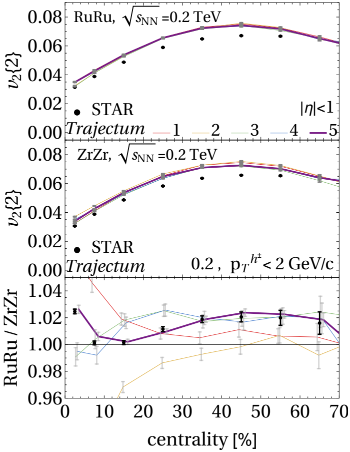

Effects of nuclear structure on soft observables

- The STAR isobar run sparked great interest in nuclear structure in heavy ion collisions.
    - Originally intended to measure the chiral magnetic effect.
- Differences in the shapes of $^{96}_{44}$Ru and $^{96}_{40}$Zr lead to different shape of the initial fireball.
    - We can distinguish several possibilities for the shapes of $^{96}_{44}$Ru and $^{96}_{40}$Zr, with model 5 giving the best agreement.
    - Isobar nature of $^{96}_{44}$Ru and $^{96}_{40}$Zr leads to robust ratios insensitive to details of hydrodynamics.

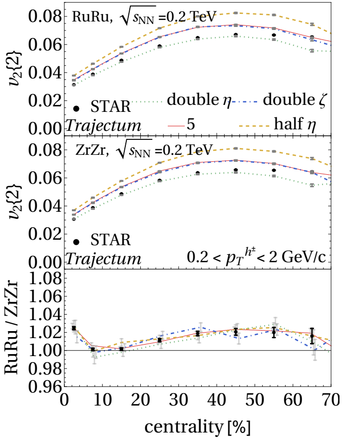

[GN, van der Schee, 2112.13771; STAR, 2109.00131]

Can we see nuclear structure without isobars?

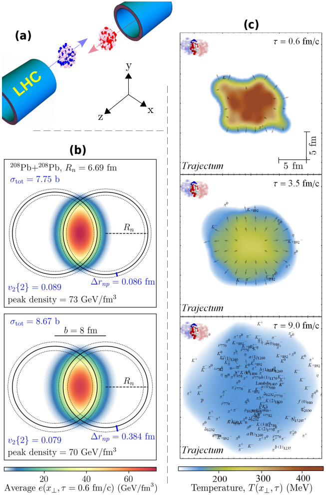

- The isobar run was particularly sensitive to nuclear structure, because other effects approximately cancel in the ratio.
- PbPb collisions at LHC energies however are not paired with anything close in mass.
- Extraction of the ^{208}Pb neutron skin from PbPb collisions alone will need to distinguish nuclear structure effects from the various model parameters.
  - Need Bayesian analysis to perform a systematic fit to take into account such correlations.

[GN, van der Schee, 2112.13771; STAR, 2109.00131]

Bayesian analysis workflow

- In principle, Bayesian analysis is simply a fit to data.
- In practice the process is more complicated:
  - Generate a large number of randomly chosen parameter sets called *design points*.
  - Run the model for each one to obtain the prior.
  - Train the emulator.
  - Run the MCMC to obtain the posterior.
- The posterior then is a list of likely parameter sets.

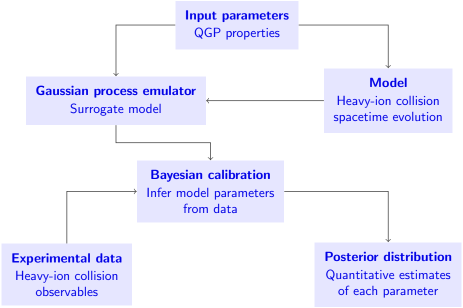

[GN, van der Schee, 2304.06191; Giacalone, GN, van der Schee, 2305.00015]

Bayesian analysis workflow

- In principle, Bayesian analysis is simply a fit to data.
- In practice the process is more complicated:
  - Generate a large number of randomly chosen parameter sets called *design points*.
  - Run the model for each one to obtain the prior.
  - Train the emulator.
  - Run the MCMC to obtain the posterior.
- The posterior then is a list of likely parameter sets.

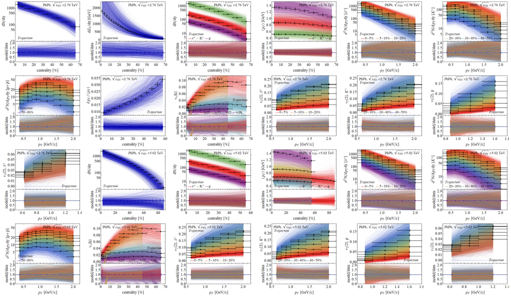

Bayesian analysis workflow

- In principle, Bayesian analysis is simply a fit to data.
- In practice the process is more complicated:
  - Generate a large number of randomly chosen parameter sets called *design points*.
  - Run the model for each one to obtain the prior.
  - Train the emulator.
  - Run the MCMC to obtain the posterior.
- The posterior then is a list of likely parameter sets.

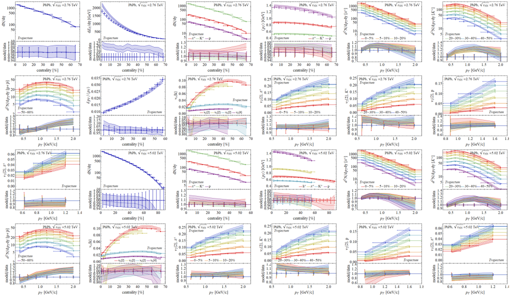

Bayesian analysis workflow

- In principle, Bayesian analysis is simply a fit to data.
- In practice the process is more complicated:
  - Generate a large number of randomly chosen parameter sets called *design points*.
  - Run the model for each one to obtain the prior.
  - Train the emulator.
  - Run the MCMC to obtain the posterior.
- The posterior then is a list of likely parameter sets.

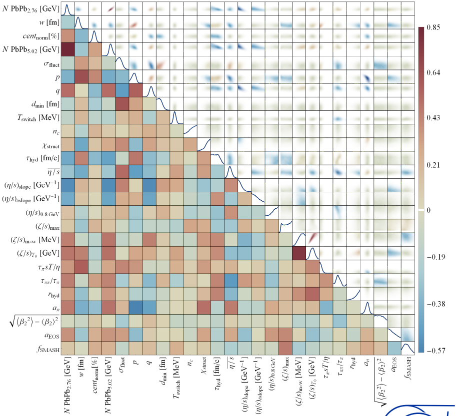

Data used: 670 individual data points

✓: data used 🕓: data available ✗: data unavailable	PbPb 2.76 TeV incl.	PbPb 2.76 TeV $\pi^\pm$	PbPb 2.76 TeV $K^\pm$	PbPb 2.76 TeV p	PbPb 5.02 TeV incl.	PbPb 5.02 TeV $\pi^\pm$	PbPb 5.02 TeV $K^\pm$	PbPb 5.02 TeV p	pPb 5.02 TeV incl.
σ	✗	✗	✗	✗	✓	✗	✗	✗	✓
dN/dy	✓	✓	✓	✓	✓	✓	✓	✓	🕓
$\langle p_T \rangle$	✗	✓	✓	✓	✓	✓	✓	✓	🕓
$dE_T/d\eta$	✓	✗	✗	✗	✗	✗	✗	✗	✗
$\delta p_T/\langle p_T \rangle$	✓	✗	✗	✗	✗	✗	✗	✗	✗
$v_{2,3,4}\{2\}$	✓	🕓	🕓	🕓	✓	🕓	🕓	🕓	🕓
$v_2\{4\}$	✓	✗	✗	✗	✓	🕓	🕓	🕓	🕓
$d^2N/dp_T dy$	✗	✓	✓	✓	✗	✓	✓	✓	✗
$v_2\{2\}(p_T)$	✗	✓	✓	✓	✗	✓	✓	✓	🕓
$v_3\{2\}(p_T)$	✗	✓	🕓	🕓	✗	✓	🕓	🕓	🕓
$NSC(2,3)$	🕓	✗	✗	✗	✓	✗	✗	✗	🕓
$NSC(2,4)$	🕓	✗	✗	✗	✓	✗	✗	✗	🕓
$\rho(v_2\{2\}^2, \langle p_T \rangle)$	✗	✗	✗	✗	✓	✗	✗	✗	✗

Uses of Bayesian analysis: viscosities

- We know the QGP phase is described by viscous hydrodynamics.
  - We know exactly what the free parameters are, i.e. η/s, ζ/s, ...
- We can use Bayesian analysis to find data-preferred values for these parameters.
- The values of the parameters provide an interface with microscopic theories of the QGP.

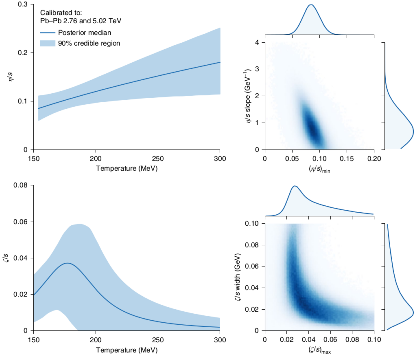

Using the posterior parameter values to make predictions

- The posterior parameter values can be used to make predictions for new observables.
  - When using multiple samples from the posterior, this includes systematic uncertainty from the parameter estimation.
- Here shown is the prediction for ultracentral $\langle p_T \rangle$.

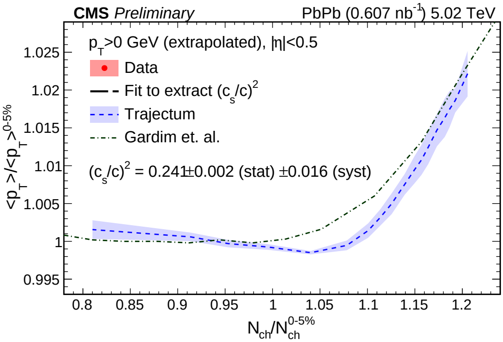

Using the posterior parameter values to make predictions

- The posterior parameter values can be used to make predictions for new observables.
  - When using multiple samples from the posterior, this includes systematic uncertainty from the parameter estimation.
- Here shown is the prediction for ultracentral $\langle p_T \rangle$.
- Precise agreement between theory and experiment.

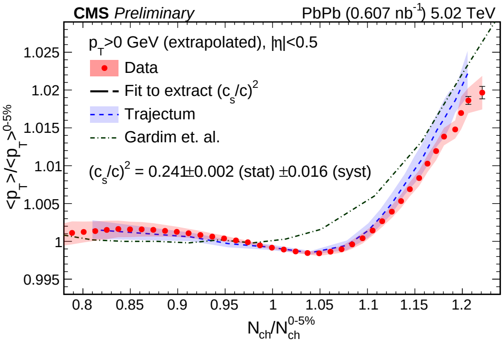

Fitting to the pPb and PbPb cross sections

- In the T$_R$ENTo model, the nucleon size is described by the Gaussian radius w.
- Previous analyses favored $w \approx 1$ fm.
  - This leads to a 3σ discrepancy in σ_{PbPb}.
- Fitting to the pPb and PbPb cross sections lowers w to 0.6 fm.
  - σ_{PbPb} discrepancy is reduced to 1σ.
  - Many other observables fit slightly worse.
- Smaller width is now compatible with our knowledge of the gluonic structure of the proton at low x.

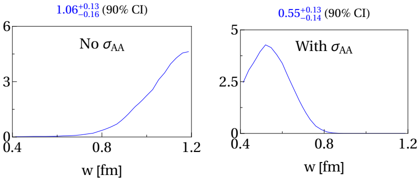

	σ_{PbPb}[b]	$\sigma_{p\mathrm{Pb}}$[b]
with σ_{AA}	8.02 ± 0.19	2.20 ± 0.06
without σ_{AA}	8.95 ± 0.36	2.48 ± 0.10
ALICE/CMS	7.67 ± 0.24	2.06 ± 0.08

[GN, van der Schee, 2206.13522; ALICE, 2204.10148; CMS, 1509.03893; Caldwell, Kowalski, *Phys. Rev. C* **81** (2010) 025203]

Energy deposition in the initial state

- Nuclear thickness functions $\mathcal{T}_{A/B}$ deposit matter into the initial state energy density $\mathcal{T}$ as follows:

$$\mathcal{T} \propto \left(\frac{\mathcal{T}_A^p + \mathcal{T}_B^p}{2} \right)^{q/p} \stackrel{p \to 0}{=} (\mathcal{T}_A \mathcal{T}_B)^{q/2}.$$

- Previous analyses implicitly set $q = 1$.
- The fit to experimental data favors $q \approx 4/3$.
  - Previous default $q = 1$ is disfavored.
  - Binary scaling $q = 2$ is ruled out.
  - $q = 4/3$ indicates that $\sqrt{\mathcal{T}_A \mathcal{T}_B}$ behaves like an entropy density.

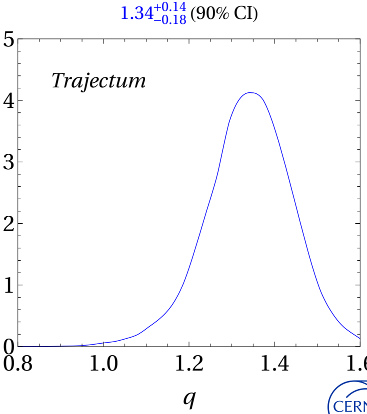

Neutron skin

- In a ^{208}Pb nucleus, neutrons sit further from the center than protons.
  - This is quantified by the *neutron skin*:

$$\Delta r_{np} = \langle r^2 \rangle_n^{1/2} - \langle r^2 \rangle_p^{1/2},$$

  i.e. the *difference* in RMS radii of the neutron and proton distributions.

- Heavy nuclei and neutron stars are sensitive to the same nuclear interactions.
  - A constraint on Δr_{np} translates directly into a constraint on the radius of a $1.4 M_\odot$ neutron star.
  - We can learn something about the low T, high μ_B region even at LHC energies!

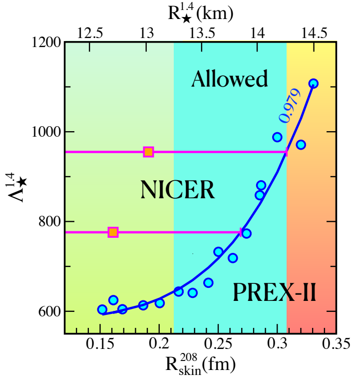

How to measure neutron skin?

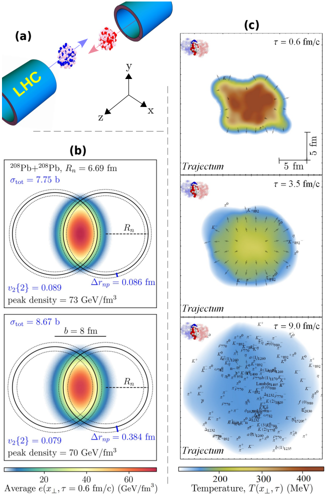

- To measure the neutron skin, we need the distributions of protons and neutrons inside the nucleus.
  - The proton distribution distribution is well-known from electron scattering.
- Several different methods are in use for the neutron distribution:
  - Polarized electron scattering off ^{208}Pb (PREX).
  - Photon tomography of ^{197}Au (STAR).
- Heavy ion collisions provide a completely orthogonal method.
  - Sensitive to the total matter distribution inside the nucleus.
  - Purely gluonic measurement.

The Woods-Saxon distribution

- Nucleon positions are drawn from a Woods-Saxon distribution:

$$\rho_{\mathrm{WS}}(r) \propto \frac{1}{1+\exp\left(\frac{r-R}{a}\right)}.$$

  - We fix R for both protons and neutrons.
  - We fix a for protons, while varying a_n as a parameter.

- Neutron skin $\Delta r_{np} = \langle r^2\rangle_n^{1/2} - \langle r^2\rangle_p^{1/2}$ strongly depends on a_n:

$$\langle r^2\rangle_{\mathrm{WS}} = \frac{12a^2\,\mathrm{Li}_5\left(-e^{R/a}\right)}{\mathrm{Li}_3\left(-e^{R/a}\right)}.$$

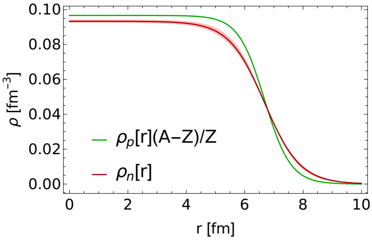

	proton	neutron
R [fm]	6.68	6.69
a [fm]	0.447	a_n

The Woods-Saxon distribution

- Nucleon positions are drawn from a Woods-Saxon distribution:

$$\rho_{WS}(r) \propto \frac{1}{1 + \exp\left(\frac{r-R}{a}\right)}.$$

  - We fix R for both protons and neutrons.
  - We fix a for protons, while varying a_n as a parameter.

- Neutron skin $\Delta r_{np} = \langle r^2 \rangle_n^{1/2} - \langle r^2 \rangle_p^{1/2}$ strongly depends on a_n:

$$\langle r^2 \rangle_{WS} = \frac{12a^2 \, \mathrm{Li}_5\left(-e^{R/a}\right)}{\mathrm{Li}_3\left(-e^{R/a}\right)}.$$

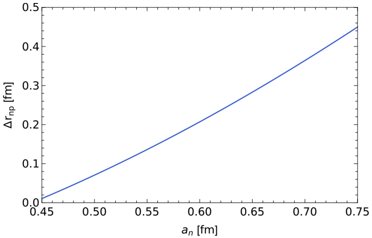

	proton	neutron
R [fm]	6.68	6.69
a [fm]	0.447	a_n

Do we have observables sensitive to a_n?

- Initial geometry is sensitive to a_n. Larger nuclei lead to:
  - Larger hadronic PbPb cross-section,
  - Larger initial QGP size,
  - Smaller initial QGP eccentricity.
- Final state observables are in turn sensitive to initial geometry. Larger Δr_{np} leads to:
  - Larger hadronic PbPb cross-section,
  - Smaller charged particle yield,
  - Smaller mean transverse momentum,
  - Smaller elliptic flow.

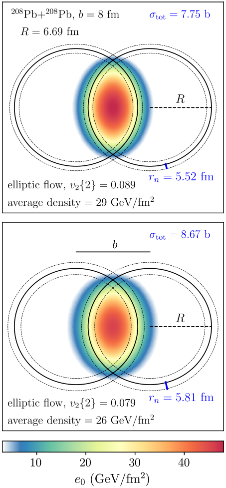

Do we have observables sensitive to a_n?

- Initial geometry is sensitive to a_n. Larger nuclei lead to:
  - Larger hadronic PbPb cross-section,
  - Larger initial QGP size,
  - Smaller initial QGP eccentricity.
- Final state observables are in turn sensitive to initial geometry. Larger Δr_{np} leads to:
  - Larger hadronic PbPb cross-section,
  - Smaller charged particle yield,
  - Smaller mean transverse momentum,
  - Smaller elliptic flow.

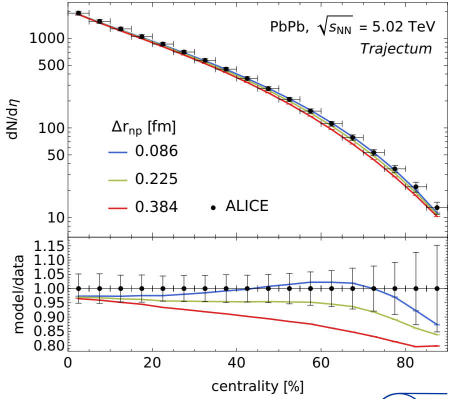

Do we have observables sensitive to a_n?

- Initial geometry is sensitive to a_n. Larger nuclei lead to:
  - Larger hadronic PbPb cross-section,
  - Larger initial QGP size,
  - Smaller initial QGP eccentricity.
- Final state observables are in turn sensitive to initial geometry. Larger Δr_{np} leads to:
  - Larger hadronic PbPb cross-section,
  - Smaller charged particle yield,
  - Smaller mean transverse momentum,
  - Smaller elliptic flow.

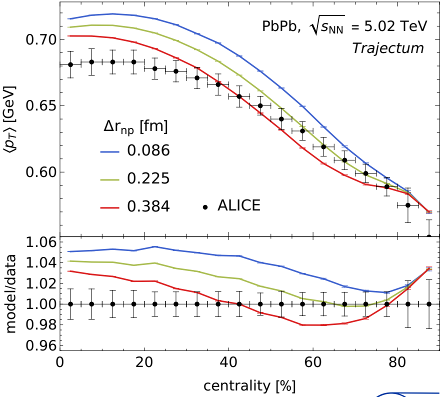

Do we have observables sensitive to a_n?

- Initial geometry is sensitive to a_n. Larger nuclei lead to:
  - Larger hadronic PbPb cross-section,
  - Larger initial QGP size,
  - Smaller initial QGP eccentricity.
- Final state observables are in turn sensitive to initial geometry. Larger Δr_{np} leads to:
  - Larger hadronic PbPb cross-section,
  - Smaller charged particle yield,
  - Smaller mean transverse momentum,
  - Smaller elliptic flow.

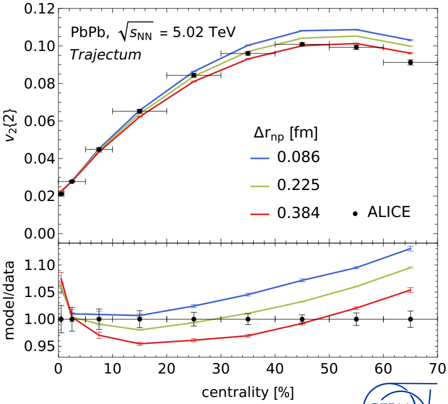

What does a_n correlate with?

- a_n is not the only parameter affecting the initial geometry, leading to correlations. a_n:
  - anticorrelates with p,
  - mildly anticorrelates with both w and q.
- Correlations highlight the importance of global analysis.
- Parameters are not degenerate, allowing us to extract a_n, and with it, Δr_{np}.

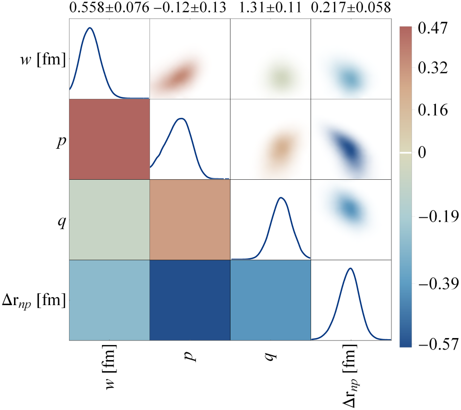

Bayesian analysis result using LHC data

- Resulting posterior for Δr_{np} is compatible with PREX II and ab initio nuclear theory.
- Slightly stronger constraint than PREX II ($\Delta r_{np} = 0.283 \pm 0.071$).
- Result is in principle improvable with better Bayesian analyses.
  - May be hard to do in practice.
  - The current analysis already took 2M CPUh.

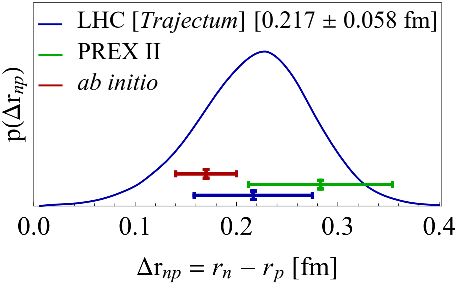

Future improvements

- We kept R_n fixed in the present analysis.
  - Bayesian analysis increases in difficulty with more parameters.
  - A priori it was not clear that this approach would work.
  - Decided to include only a_n in the first analysis.
- What can be expected from varying R_n in a future Bayesian analysis?
  - When varying R_n, as R_n grows, σ_{PbPb} increases and $\langle p_T \rangle$ decreases.
  - Smallness of of σ_{PbPb} prefers smaller R_n, possibly leading to a smaller estimate of Δr_{np}.
  - In this case bulk viscosity would need to increase to compensate for $\langle p_T \rangle$.

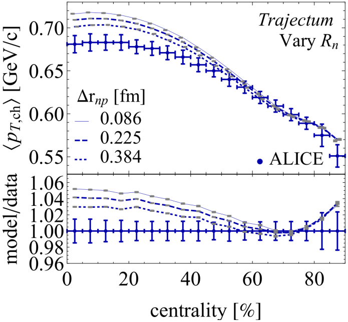

The deformation of ^{129}Xe

- We describe ^{129}Xe with a *deformed* Woods-Saxon distribution:

$$\rho_{WS}(r) \propto \frac{1}{1+\exp\left(\frac{r-R(\theta,\phi)}{a}\right)},$$

$$R(\theta,\phi) = R\left(1+\beta_2\cos\gamma\, Y_2^0 + \beta_2 \sin\gamma\, Y_2^2\right),$$

with Y_l^m spherical harmonics.

  - We do not distinguish protons and neutrons.

- Observables in the central region are sensitive to β_2 and γ:
  - v_2 is sensitive to β_2.
  - ρ_2 is sensitive to β_2 and γ.

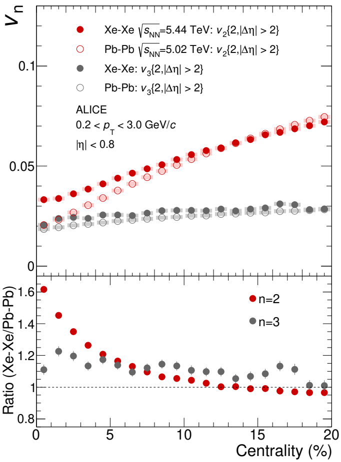

The deformation of ^{129}Xe

- We describe ^{129}Xe with a *deformed* Woods-Saxon distribution:

$$\rho_{\mathrm{WS}}(r) \propto \frac{1}{1+\exp\left(\frac{r-R(\theta,\phi)}{a}\right)},$$

$$R(\theta,\phi) = R\left(1+\beta_2 \cos\gamma\, Y_2^0 + \beta_2 \sin\gamma\, Y_2^2\right),$$

  with Y_l^m spherical harmonics.
  - We do not distinguish protons and neutrons.
- Observables in the central region are sensitive to β_2 and γ:
  - v_2 is sensitive to β_2.
  - ρ_2 is sensitive to β_2 and γ.

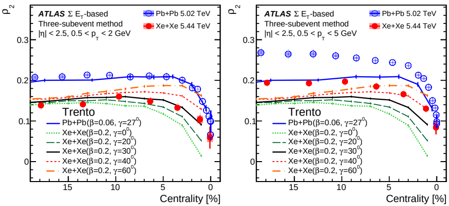

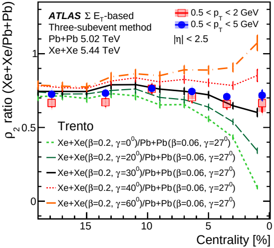

[Giacalone, GN, van der Schee, xxxx.xxxxx; ALICE, 1805.01832; ATLAS, 2205.00039]

Bayesian analysis result using LHC data

- We are able to extract the skin depth a.
  - Ab initio PGCM calculations yield $a = 0.492$ fm.
- The deformation parameters β_2 and γ are well constrained.
  - PGCM gives $\beta_2 = 0.207$ and $\gamma = 26.93^\circ$.
- We can access all kinds of shape information, not just neutron skin!
- The nucleus ^{229}Th is interesting for BSM physics. Main theory uncertainty is its β_2.

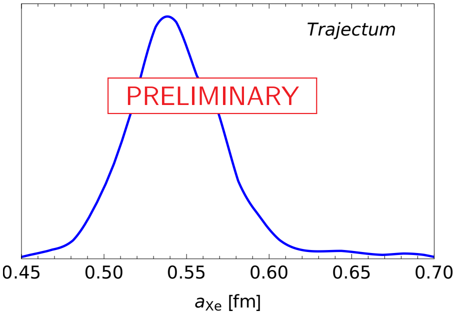

[Giacalone, GN, van der Schee, xxxx.xxxxx; Bally, Bender, Giacalone, Somà, 2108.09578; Caputo et al., 2407.17526]

Bayesian analysis result using LHC data

- We are able to extract the skin depth a.
  - Ab initio PGCM calculations yield $a = 0.492$ fm.
- The deformation parameters β_2 and γ are well constrained.
  - PGCM gives $\beta_2 = 0.207$ and $\gamma = 26.93^\circ$.
- We can access all kinds of shape information, not just neutron skin!
- The nucleus ^{229}Th is interesting for BSM physics. Main theory uncertainty is its β_2.

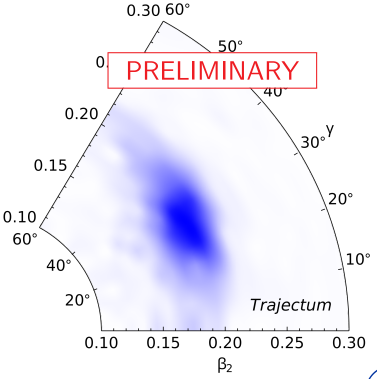

Backup

Backup

Bayesian analysis details

- 3000 design points.
- 18k events per design point.
- Every 15th design point has 10× more statistics, enabling to emulate 'hard' observables such as $SC(n, m)$ and $\rho(v_2\{2\}^2, \langle p_T \rangle)$.

Error budget

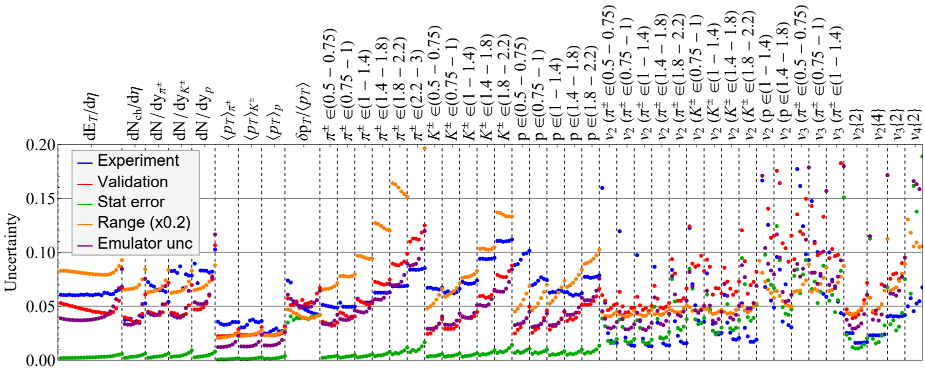

Posterior observables (1/3)

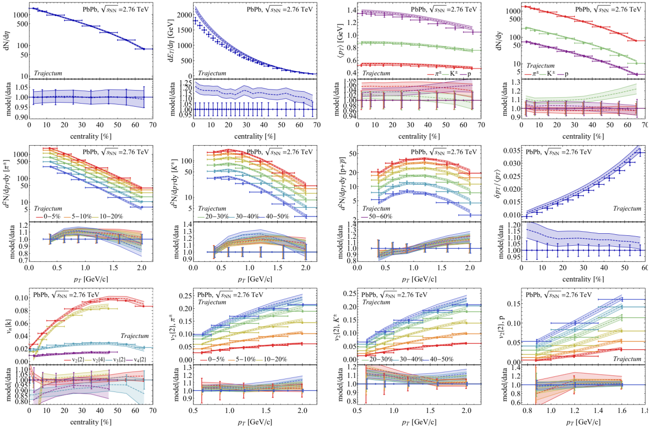

Posterior observables (2/3)

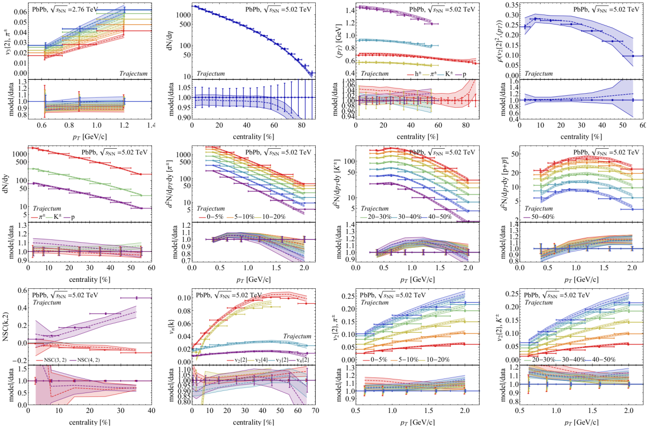

Posterior observables (3/3)

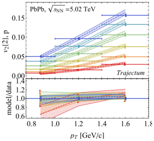

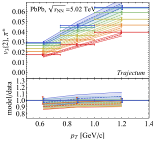

TRENTo initial conditions

- Nucleons A and B become *wounded* with probability

$$P_{\text{wounded}} = 1 - \exp\left(-\sigma_{gg}\int d\mathbf{x}\,\rho_A(\mathbf{x})\rho_B(\mathbf{x})\right), \quad \rho_A \propto \exp\left(\frac{-|\mathbf{x}-\mathbf{x}_A|^2}{2w^2}\right).$$

- Each wounded nucleon desposits energy into its nucleus's *thickness function* $\mathcal{T}_{A/B}$:

$$\mathcal{T}_{A/B} = \sum_{i\in\text{wounded A/B}} \gamma\exp(-|\mathbf{x}-\mathbf{x}_i|^2/2w^2),$$

  with γ drawn from a gamma distribution with mean 1 and standard deviation σ_{fluct}.

- Actual formulas slightly modified because each nucleon has n_c constituents.

The TRENTo phenomenological ansatz

- The standard TRENTo formula combines thickness functions of the two nuclei $\mathcal{T}_A$ and $\mathcal{T}_B$ into a *reduced thickness* $\mathcal{T}$, interpreted as an energy density:

$$\mathcal{T} \propto \left(\frac{\mathcal{T}_A^p + \mathcal{T}_B^p}{2} \right)^{1/p},$$

  with p a parameter.

- Some useful limits:

p	-1	0	1
$\mathcal{T}$	$\frac{2}{\frac{1}{\mathcal{T}_A}+\frac{1}{\mathcal{T}_B}}$	$\sqrt{\mathcal{T}_A\mathcal{T}_B}$	$\frac{\mathcal{T}_A+\mathcal{T}_B}{2}$

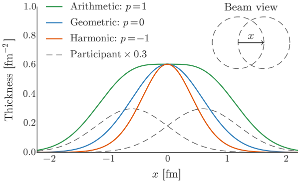

Free streaming pre-hydrodynamic stage

- TRENTo creates matter at proper time $\tau = 0^+$.
- Propagate the matter using free streaming:

$$T^{\mu\nu}(x, y, \tau_{\text{hyd}}) = \frac{1}{\tau_{\text{hyd}}} \int d\phi\, \hat{p}^\mu \hat{p}^\nu \mathcal{T}(x - \tau_{\text{hyd}} \cos\phi, y - \tau_{\text{hyd}} \sin\phi),$$

with

$$\hat{p}^\mu = \begin{pmatrix} 1 & \cos\phi & \sin\phi \end{pmatrix},$$

giving us the stress tensor $T^{\mu\nu}$ at proper time $\tau = \tau_{\text{hyd}}$.

- Here τ_{hyd} is the time at which hydrodynamics is started.
- The factor $1/\tau_{\text{hyd}}$ is due to longitudinal expansion.

Basics of hydrodynamics

- Hydrodynamics is the ultimate effective theory. Knowledge of the underlying microscopic theory is completely summarized in transport coefficients.
- Only conservation laws survive: equation of motion is simply

$$\partial_\mu T^{\mu\nu} = 0.$$

- Not enough equations to close the system. Need additional assumption of *local thermal equilibrium*.
- We write $T^{\mu\nu}$ in terms of building blocks T, u^μ, $g^{\mu\nu}$ and ∂_μ.

[Kovtun, 1205.5040; Glorioso, Liu, 1805.09331]

Hydrodynamics in the 14-moment approximation

- Define ($g^{\mu\nu} = \mathrm{diag}(1, -1, -1, -1)$):

$$\Delta^{\mu\nu} = g^{\mu\nu} - u^\mu u^\nu, \quad \nabla^\mu = \Delta^{\mu\nu}\partial_\nu, \quad D = u^\mu \nabla_\mu, \quad \sigma^{\mu\nu} = \nabla^{\langle\mu} u^{\nu\rangle},$$

  with $\langle\rangle$ symmetrizing and removing the trace.

- We solve viscous hydrodynamics without currents, i.e.

$$\partial_\mu T^{\mu\nu} = 0, \quad T^{\mu\nu} = eu^\mu u^\nu - (P + \Pi)\Delta^{\mu\nu} + \pi^{\mu\nu},$$

- $\pi^{\mu\nu}$ and Π follow the 14-moment approximation:

$$\begin{aligned} -\tau_\pi \Delta^\mu_\alpha \Delta^\nu_\beta D\pi^{\alpha\beta} &= \pi^{\mu\nu} - 2\eta\sigma^{\mu\nu} + \delta_{\pi\pi}\pi^{\mu\nu}\nabla\cdot u \\ &\quad - \phi_7 \pi_\alpha^{\langle\mu}\pi^{\nu\rangle\alpha} + \tau_{\pi\pi}\pi_\alpha^{\langle\mu}\sigma^{\nu\rangle\alpha} - \lambda_{\pi\Pi}\Pi\sigma^{\mu\nu}, \\ -\tau_\Pi D\Pi &= \Pi + \zeta\nabla\cdot u + \delta_{\Pi\Pi}\nabla\cdot u\Pi - \lambda_{\Pi\pi}\pi^{\mu\nu}\sigma_{\mu\nu}. \end{aligned}$$

[Denicol, Jeon, Gale, 1403.0962]

Particlization

- At the freeze-out temperature T_{sw}, we turn the fluid back into particles.
- Particles are sampled thermally, and boosted with the fluid velocity u^μ.
- We use the PTB prescription to match $\pi^{\mu\nu}$ and Π across the transition, so that $T^{\mu\nu}$ is smooth.
- After particlization, we use SMASH as a hadronic afterburner.

[Pratt, Torrieri, 1003.0413; Bernhard, 1804.06469; Weil et al., 1606.06642, Sjostrand, Mrenna, Skands, 0710.3820]

Nucleon width and $\rho(v_n\{2\}^2, \langle p_T \rangle)$

- Previous study shows that $\rho(v_n\{2\}^2, \langle p_T \rangle)$ depends strongly on the nucleon size w.

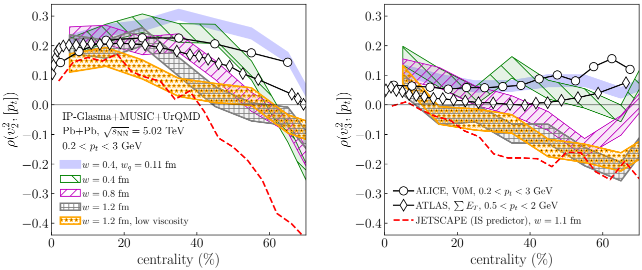

Why weights?

- Higher p_T, higher centralities are harder to model theoretically.
- Experimental correlation matrix is not available.
    - Figure shows 1σ and 2σ regions for $\rho \in \{0, 0.9, -0.9, 0.99\}$, with standard deviations the same.
    - Same difference between theory and experiment can be within 1σ or outside of 2σ depending on ρ.
    - Correlated observable classes can be over/underimportant for the Bayesian analysis.

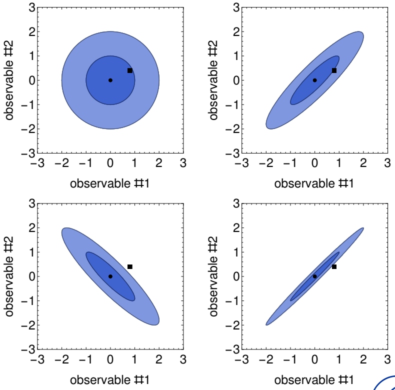

Definition of weights

- In the bayesian analysis, the probability of the data given the parameter point x is given by:

$$P(D|x) = \frac{1}{\sqrt{(2\pi)^m \det \Sigma}} \exp\left(-\frac{1}{2}(y - y_{\text{exp}})^T \Sigma^{-1} (y - y_{\text{exp}})\right),$$

  with y the vector of observables computed from x, y_{exp} the vector of the corresponding experimental data, and Σ the combined theory/experiment covariance matrix.

- We define weights by replacing

$$P(D|x) = \frac{1}{\sqrt{(2\pi)^m \det \Sigma}} \exp\left(-\frac{1}{2}(y - y_{\text{exp}})^T \omega \Sigma^{-1} \omega (y - y_{\text{exp}})\right),$$

  where ω is the diagonal matrix containing the weight for each observable.

Choice of weights

- We choose for weights ω:
  - 1/2 for every particle identified observable.
  - 1/2 for p_T-differential observables, and an additional $(2.5 - p_T[\text{GeV}])/1.5$ if $p_T > 1\,\text{GeV}$.
  - $(100 - c[\%])/50$ if the centrality class c is beyond 50%.
- Weighting only worsens the average discrepancy slightly.
- Distribution of discrepancies makes more sense.

	$\langle(y_{\text{theory}} - y_{\text{experiment}})/\sigma\rangle$				$\bar{\omega}$
	σ_{AA} & ω	ω	σ_{AA}	neither	
$dN_{ch}/d\eta$	0.55	0.60	1.23	1.22	1.00
$dN_{\pi^\pm,k^\pm,p^\pm}/dy$	0.76	0.70	0.60	0.57	0.48
$dE_T/d\eta$	1.59	1.51	0.82	0.77	0.48
$\langle p_T\rangle_{ch,\pi^\pm,K^\pm,p^\pm}$	0.66	0.60	0.88	0.72	0.46
$\delta p_T/\langle p_T\rangle$	0.56	0.62	0.51	0.58	0.49
$v_n\{k\}$	0.58	0.51	0.54	0.49	1.00
$d^2N_{\pi^\pm}/dy\,dp_T$	1.19	1.07	0.86	0.92	0.20
$d^2N_{K^\pm}/dy\,dp_T$	1.41	1.27	0.79	0.73	0.20
$d^2N_{p^\pm}/dy\,dp_T$	1.35	1.21	0.73	0.67	0.25
$v_2^{\pi^\pm}(p_T)$	0.81	0.74	0.46	0.44	0.19
$v_2^{K^\pm}(p_T)$	0.92	0.89	0.55	0.55	0.19
$v_2^{p^\pm}(p_T)$	0.49	0.47	0.34	0.35	0.25
$v_3^{\pi^\pm}(p_T)$	0.65	0.57	0.69	0.57	0.24
average	0.89	0.83	0.69	0.66	
σ_{AA}	1.13	3.80	1.53	3.40	1.00

How much do weights change the posteriors?